

Performance Analysis of a Floating Hollow Cylindrical Break water in Experimental Study

El Saie, Y.M.

Associate Professor Dr. Yasser Sadek El Saie, Head of Civil Engineering Department in the Higher Institute of Engineering, El Shorouk City, Cairo, Egypt
Corresponding Author: El Saie, Y.M.

Abstract: *The objective of the present study is to investigate the performance of a floating hollow cylindrical breakwater system based on experimental laboratory tests. These experiments were carried out in a recirculating open channel flume located in the Hydraulics Laboratory at Higher Institute of Engineering in El Shorouk City. The physical model consists of five models of different diameters (2, 3, 4, (3&4) and (2,3&4) inches), horizontal hollow cylindrical floating pipes worked as floating breakwater, tested as a single then as a group. In every case the incident and transmitted wave heights can be measured with system of wireless Sonic Wave Sensor, then wave coefficients (C_t , C_r and C_d) can be calculated, also the percentage of transmitted energy can be calculated to evaluate the performance of these models.*

Date of Submission: 25-05-2019

Date of acceptance: 10-06-2019

I. Introduction

Breakwaters are used to provide sheltered areas for loading or unloading of ships, either coastal protection. Often the breakwaters are bottom mounted such as rubble mound breakwaters. However, there can be several advantages using a Floating Breakwater. For instance, they can be moved to second location with nearly little effort. Also when the water depth increases, the costs of a bottom-mounted breakwater increase substantially, which leads to the floating breakwater concept economically attractive. Further, if the soil conditions are not suited for high loads, a Floating Breakwater might be the only solution to attenuate the incoming wave field.

The use of Floating Breakwaters can get an enhanced attention in the coming years due to an anticipated development of the Sea space by **Christensen et al., (2015)**. Infrastructure makes the concept of multi-use offshore platforms particularly interesting, where floating breakwaters can play very important role in protecting service platforms and offshore terminals. **Sannasiraj et al., (1998)**, studied a single pontoon breakwater experimentally and theoretically. **Abul-Azm and Gesraha, (2000) and Gesraha, (2006)**, studied the hydrodynamics based on oblique waves. **Koutandos et al., (2004)** developed a Boussinesq model coupled with a 2DV elliptical model to study the hydrodynamic behavior of fixed and heave motion FBs. **Rahman et al., (2006)**, studied the single pontoon breakwater with a VOF-type Navier-Stokes solver for the original introduction to VOF-method. For instance **Dong et al., (2008)**, studied different configurations of partly open breakwaters, i.e. single-box FB, double-box FB, and board-net floating breakwaters.

Ji et al., (2015) and Ji et al., (2016) used experiments to optimize the configuration of FBs. They found that a FB consisting of two pontoons with amesh between them gave the best performance in wave attenuation. Further, they suggested that this could be combined with porous structures in order to improve the functionality of the structure. **Tang et al., (2011)**, presented another dual pontoon floating structure, where the pontoons supported a fish net for aquaculture. In this case the fish net acts as a very open porous structure, which in **Wang and Sun, (2010)** was found to increase the wave attenuation caused by energy dissipation.

Examples of full three-dimensional studies of floating breakwaters can for instance be found in **Loukogeorgaki and Angelides, (2005) and Loukogeorgaki et al., (2014)**.

This paper presents experimental analysis of the motion of a five models of Floating Breakwater, and its reflection, dissipation and transmission of wave energy. The basic geometry of the cross section of the physical model was based on a single pipe with different diameters (2, 3 & 4 inch) rested on a floating base, fourth model of two pipes together (3 & 4 inch together) and finally the fifth model (2&3&4 inch together). The objective of this paper is to study the effect of using these different physical models as a floating Breakwater, and how they influence the dissipation, reflection and transmission of waves.

II. Experimental Work

The tests were carried out in a wave flume in the Hydraulic laboratory at the Higher Institute of Engineering, in El Shorouk City. The flume is 12.00 m long, 0.50 m wide, and the sidewalls are 0.60 m high, see Fig. (1). The sidewalls of the flume consisted of a 12.00 panels of glass each one meter, to enable for following the motion of the Floating Breakwater as shown in figure (2). The flume was equipped with a piston-type wave maker at one end and a wave absorber before it and a wave absorber at the other side of the flume. The water depth in the flume was fixed to 30 cm, as a maximum water depth in the flume. Wave period and wave length are measured by Sonic Wave Sensor XB as shown in figure (3).



Fig. (1). General View of the Wave Flume

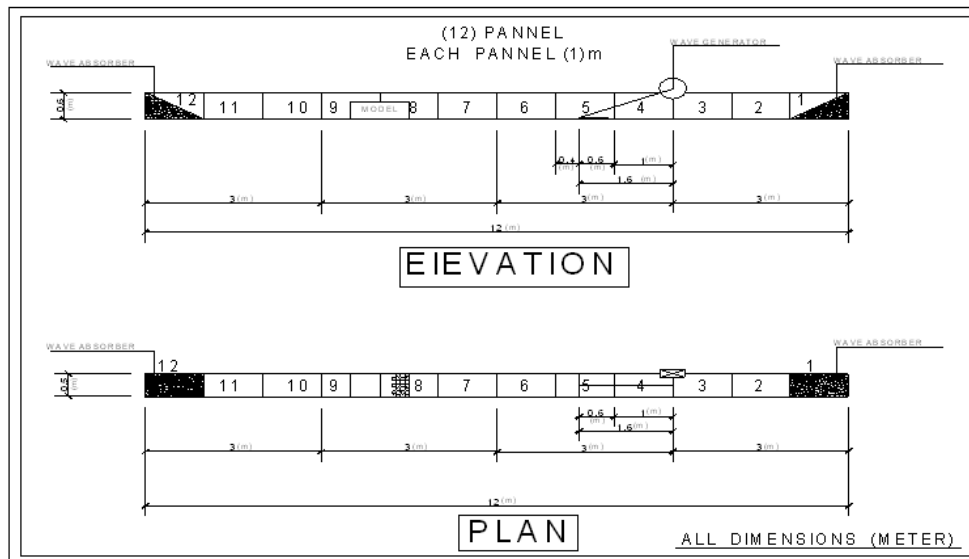


Fig. (2) Layout of the Flume

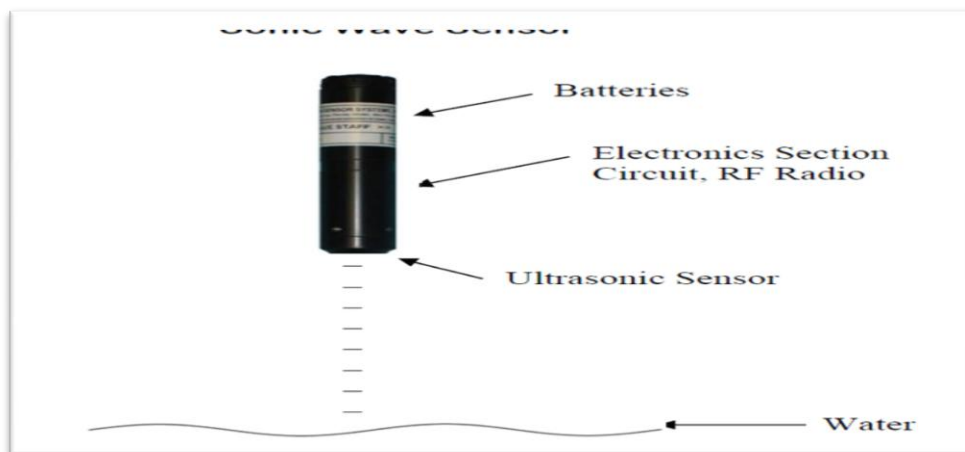


Fig. (3) Photo of Sonic Wave Sensor

Design of the Physical models

The physical model consists of five models of a hollow cylindrical horizontal floating pipes with different diameters (2, 3, 4, (3&4) and (2&3&4) inch) rested on a wooden floating base which tied at the base of the flume by some anchors, with dimensions of 45 cm long, 16 cm width and 7 cm height. The horizontal pipe hanging over two vertical sides of height 14 cm. Water depth was constant at 30 cm) with different wave heights, lengths and periods. By testing these models separately and by connecting each other's to evaluate the performance of each model for dissipate the incident wave energy and also to calculate wave coefficients (C_t , C_r and C_d), also the maximum possible transmitted energy. Finally, the steps of manufacturing these models as shown in the following figures (4, 5, 6, 7, 8, 9, & 10).



Fig.(4) Three pipes and their bases



Fig. (5) Models after adding stiffeners



Fig. (6) First model with $\varnothing = 2$ inch



Fig. (7) Second model with $\varnothing = 3$ inches



Fig. (8) Third model with $\varnothing = 4$ inches



Fig. (9) Fourth model $\varnothing = 3$ & 4 inches



Fig. (10) Fifth model with $\varnothing = 2, 3$ & 4 inches

Measurements and Results

By experiment these models in the flume and measure the wave heights by Sonic Wave Sensor XB before and after the tested models, these measurements and calculated coefficients (Ct, Cr & Cd) are tabulated in the following tables (1, 2, 3, 4 &5).

Table (1) Measured and calculated data for $\varnothing = 2$ inch

Hi(cm)	Ht (cm)	Hr (cm)	Length (cm)	T (sec)	Hi/L	Ct	Cr	Cd	% Energy transmitted
10.06	8.83	0.24	139.37	0.946	0.0722	0.8777	0.0239	0.4786	77.04
9.01	7.87	0.23	122.339	0.867	0.0736	0.8813	0.0252	0.4719	76.59
7.96	6.721	0.21	106.548	0.827	0.0747	0.8125	0.0264	0.5824	71.29
7.34	6.12	0.19	90.231	0.762	0.0813	0.7855	0.0262	0.6183	71.30
6.15	5.07	0.17	69.254	0.664	0.0888	0.7569	0.0276	0.6530	67.96

Table (2) Measured and calculated data for $\varnothing = 3$ inch

Hi(cm)	Ht(cm)	Hr(cm)	Length (cm)	T (sec)	Hi/L	Ct	Cr	Cd	% Energy transmitted
10.06	8.35	0.01	139.37	0.946	0.0722	0.8300	0.0014	0.5577	68.89
9.01	7.315	0.01	122.339	0.867	0.0736	0.8119	0.0016	0.5838	65.91
7.96	6.321	0.01	106.548	0.827	0.0747	0.7941	0.0018	0.6078	63.06
7.34	5.65	0.01	90.231	0.762	0.0813	0.7698	0.0019	0.6383	59.25
6.15	4.56	0.01	69.254	0.664	0.0888	0.7415	0.0023	0.6710	54.98

Table (3) Measured and calculated data for $\varnothing = 4$ inch

Hi(cm)	Ht (cm)	Hr (cm)	Length (cm)	T (sec)	Hi/L	Ct	Cr	Cd	% energy transmitted
10.06	8.17	0.27	139.37	0.946	0.0722	0.8121	0.0264	0.5829	65.96
9.01	7.124	0.25	122.339	0.867	0.0736	0.7907	0.0278	0.6116	62.52
7.96	6.174	0.24	106.548	0.827	0.0747	0.7756	0.0296	0.6305	60.16
7.34	5.325	0.22	90.231	0.762	0.0813	0.7255	0.0294	0.6876	52.63
6.15	4.154	0.20	69.254	0.664	0.0888	0.6754	0.0318	0.7367	45.62

Table (4) Measured and calculated data for $\varnothing = 3$ & 4 inch (together).

Hi(cm)	Ht (cm)	Hr (cm)	Length (cm)	T (sec)	Hi/L	Ct	Cr	Cd	% energy transmitted
10.06	5.21254	0.29	139.37	0.946	0.0722	0.5181	0.0284	0.8548	26.85
9.01	4.65874	0.27	122.339	0.867	0.0736	0.5171	0.0301	0.8554	26.74
7.96	3.89754	0.26	106.548	0.827	0.0747	0.4896	0.0321	0.8713	23.97
7.34	3.45487	0.24	90.231	0.762	0.0813	0.4707	0.0321	0.8817	22.15
6.15	2.895478	0.22	69.254	0.664	0.0888	0.4708	0.0351	0.8815	22.17

Table (5) Measured and calculated data for $\varnothing = 2, 3$ & 4 inch (together).

Hi(cm)	Ht (cm)	Hr (cm)	Length (cm)	T (sec)	Hi/L	Ct	Cr	Cd	% energy transmitted
10.06	4.6875	0.32	139.37	0.946	0.0722	0.4660	0.0319	0.8842	21.71
9.01	4.01547	0.31	122.339	0.867	0.0736	0.4457	0.0340	0.8946	19.86
7.96	3.45876	0.29	106.548	0.827	0.0747	0.4345	0.0366	0.8999	18.88
7.34	3.102547	0.27	90.231	0.762	0.0813	0.4227	0.0369	0.9055	17.87
6.15	2.545875	0.25	69.254	0.664	0.0888	0.4140	0.0408	0.9094	16.25

The results of these experiments can be lustrated in few curves showing the varieties of the relations between these variables and coefficients of wave to be judge in the performance of these tested models and choose any of them to be comfortable for the purpose of use.

Also figures (11, 12, 13, 14 & 15) shows the relations between wave steepness Hi/L and coefficient of dissipation Cd, reflected Cr & transmitted Ct for the different five tested models.

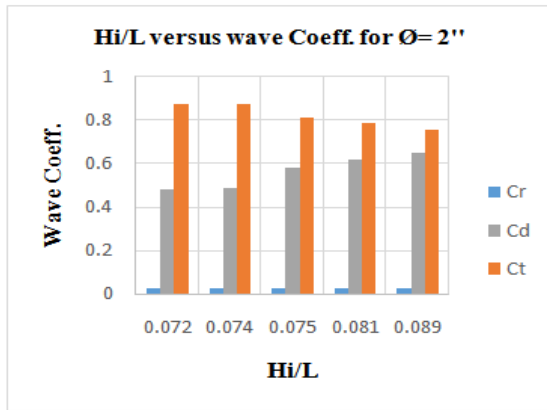


Fig. (11) Hi/L versus Cr, Cd, & Ct for Ø = 2''

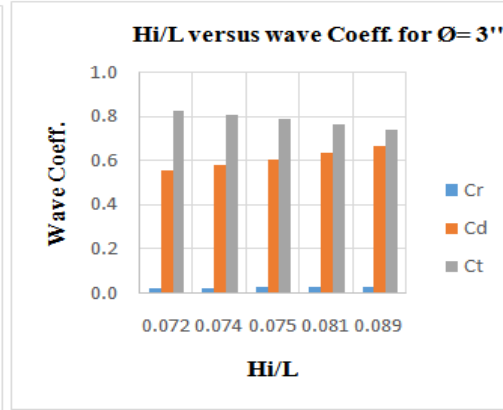


Fig.(12) Hi/L versus Cr, Cd, & Ct for Ø = 3''

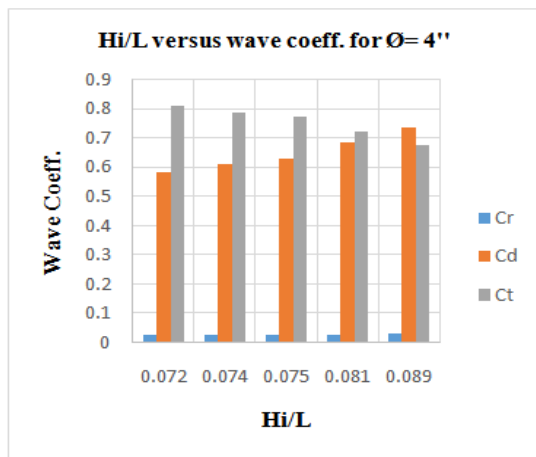


Fig. (13) Hi/L versus Cr, Cd, & Ct for Ø = 4''

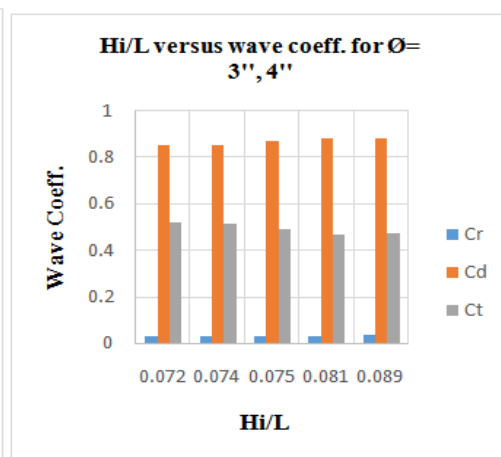


Fig. (14) Hi/L versus Cr, Cd, & Ct for Ø=3'', 4''

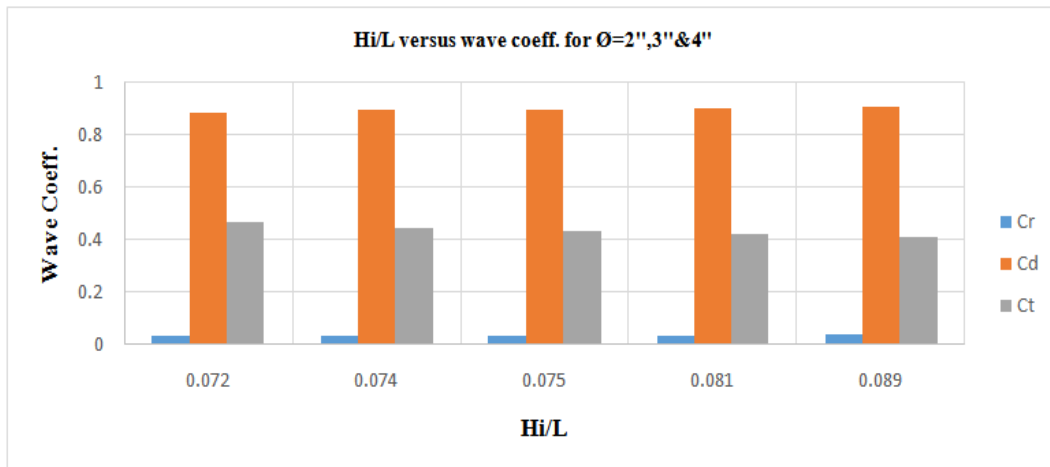


Fig. (15) Hi/L versus Cr, Cd, & Ct for Ø= 2'', 3'' & 4'' (together)

Also figures (16, 17 and 18) describe the relations between (Hi/d) and the wave coefficients Cd, Cr and Ct for the different five models of different diameters.

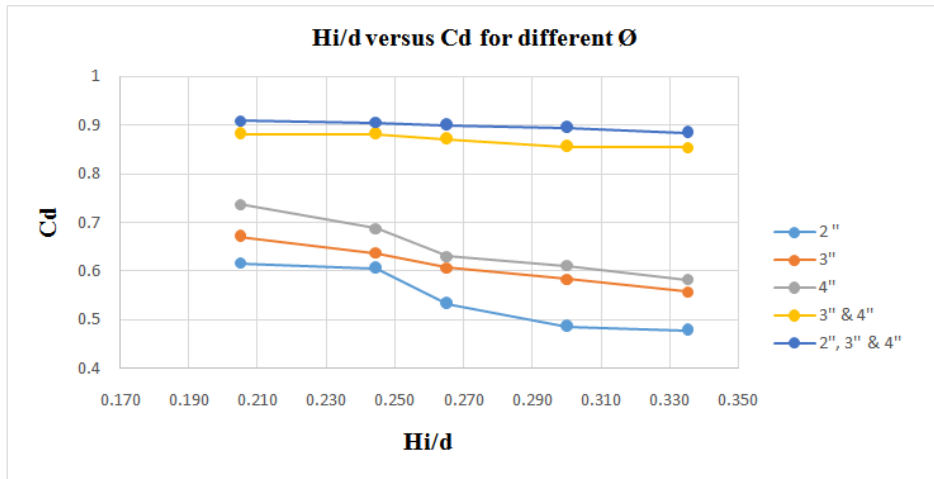


Fig. (16) Hi/d versus Cd for different models

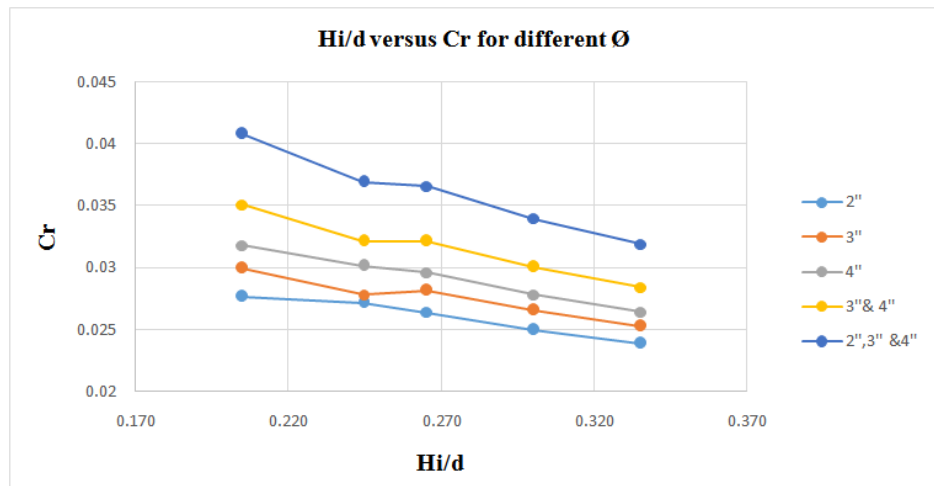


Fig. (17) Hi/d versus Cr for different models

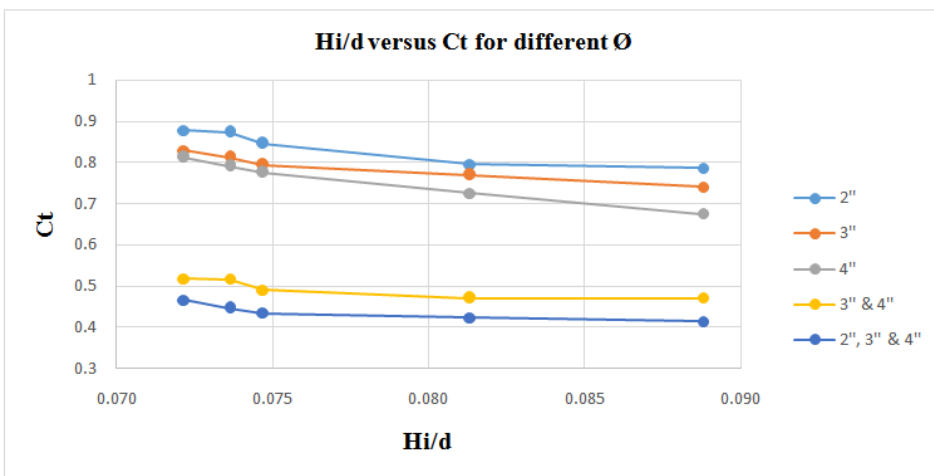


Fig. (18) Hi/d versus Ct for different models

For a comparison of percentage of energy transmitted for the five models and (H/d), figure (19) explain the difference of the five models.

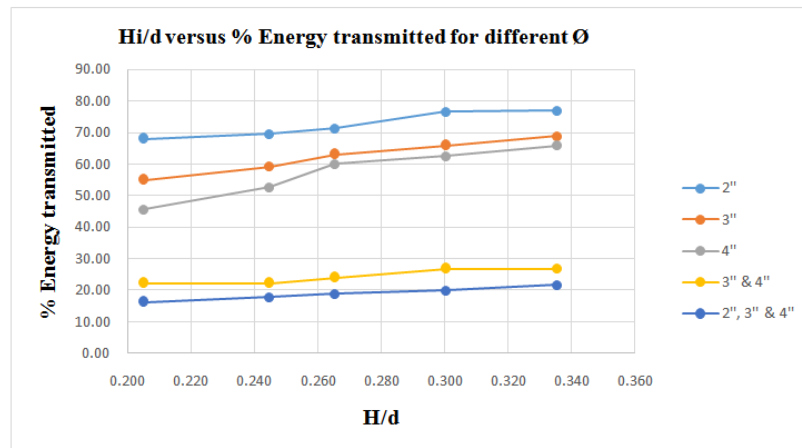


Fig. (19) Hi/d versus % energy transmitted for different models

III. Conclusions And Recommendations

The main conclusions of this paper are as follows:

- The coefficient of dissipation C_d increases gradually with the increase of diameter of the models (directly proportional), also the coefficient of transmitted C_t decreases with the increase of diameter of the models.
- The percentage of energy transmitted decreases with the increase of model diameter (inversely proportional), approximately model four and five more effective for wave energy transmission by minimum 22% to maximum 38 %.
- The difference in percentage of energy transmitted for model four and five was nearly small within 5 %, so we can use model four instead of model five for economical stage.
- The difference of changing (C_d) between model 1, 2 and 3 is nearly 11%.
- Model four or five has coefficient of dissipation C_d more than model one by nearly 35 %.

For recommended further study, a percentage of porosity in the models must be added to know the difference between the solid pipes, and add a system to these models to try generating electric energy from wave energy.

References

- [1]. Christensen, E.D., Stuiiver, M., Guanche, R., Møhlenberg, F., Schouten, J.-J., Svenstrup Pedersen, O., He, W., Zanuttigh, B., Koundouri, P., 2015. Go Offshore – Combining Food and Energy Production. Technical University of Denmark. Department of Mechanical Engineering, Kgs. Lyngby, Denmark.
- [2]. Sannasiraj, S.A., Sundar, V., Sundaravivelu, R., 1998. Mooring forces and motion responses of pontoon-type floating breakwaters. *Ocean Eng.* 25, 27–48.
- [3]. Abul-Azm, A.G., Gesraha, M.R., 2000. Approximation to the hydrodynamics of floating pontoons under oblique waves. *Ocean Eng.* 27, 365–384.
- [4]. Gesraha, M.R., 2006. Analysis of shaped floating breakwater in oblique waves: Impervious rigid wave boards. *Appl. Ocean Res.* 28, 327–338.
- [5]. Koutandos, E.V., Karambas, T.V., Koutitas, C.G., 2004. Floating breakwater response to wave's action using a Boussinesq model coupled with a 2DV elliptic solver. *J. Waterw. Port. Coast. Ocean Eng.* 130, 243–255.
- [6]. Rahman, M.A., Mizutani, N., Kawasaki, K., 2006. Numerical modeling of dynamic responses and mooring forces of submerged floating breakwater. *Coast Eng.* 53, 799–815.
- [7]. Dong, G.H., Zheng, Y.N., Li, Y.C., Teng, B., Guan, C.T., Lin, D.F., 2008. Experiments on wave transmission coefficients of floating breakwaters. *Ocean Eng.* 35, 931–938.
- [8]. Ji, C.Y., Chen, X., Cui, J., Yuan, Z.M., Incecik, A., 2015. Experimental study of a new type of floating breakwater. *Ocean Eng.* 105, 295–303.
- [9]. Ji, C.-Y., Chen, X., Cui, J., Gaidai, O., Incecik, A., 2016. Experimental study on configuration optimization of floating breakwaters. *Ocean Eng.* 117, 302–310.
- [10]. Tang, H.-J., Huang, C.-C., Chen, W.-M., 2011. Dynamics of dual pontoon floating structure for cage aquaculture in a two-dimensional numerical wave tank. *J. Fluid Struct.* 27, 918–936.
- [11]. Wang, H.Y., Sun, Z.C., 2010. Experimental study of a porous floating breakwater. *Ocean Eng.* 37, 520–527.
- [12]. Loukogeorgaki, E., Angelides, D.C., 2005. Stiffness of mooring lines and performance of floating breakwater in three dimensions. *Appl. Ocean Res.* 27, 187–208.
- [13]. Loukogeorgaki, E., Yagci, O., SedatKabdasi, M., 2014. 3D Experimental investigation of the structural response and the effectiveness of a moored floating breakwater with flexibly connected modules. *Coast Eng.* 91, 164–180.

El Saie, Y.M.. "Performance Analysis of a Floating Hollow Cylindrical Break water in Experimental Study." *IOSR Journal of Mechanical and Civil Engineering (IOSR-JMCE)*, vol. 16, no. 3, 2019, pp. 01-07